Proceedings of the 7th International Symposium on Cavitation
CAV2009 – Paper No. 36
August 17-22, 2009, Ann Arbor, Michigan, USA

Thermodynamic Effects on Cryogenic Cavitating Flow in an Orifice

Kazuki Niiyama
Japan Aerospace Exploration Agency
1 Koganesawa, Kimigaya, Kakuda,
Miyagi 981-1525, Japan
niiyama.kazuki@jaxa.jp

Satoshi Hasegawa
Japan Aerospace Exploration Agency
1 Koganesawa, Kimigaya, Kakuda,
Miyagi 981-1525, Japan
hasegawa.satoshi@jaxa.jp

Shinichi Tsuda
Japan Aerospace Exploration Agency
2-1-1 Sengen, Tsukuba,
Ibaraki 305-8505, Japan
tsuda.shinichi@jaxa.jp

Yoshiki Yoshida
Japan Aerospace Exploration Agency
1 Koganesawa, Kimigaya, Kakuda,
Miyagi 981-1525, Japan
yoshida.yoshiki@jaxa.jp

Tsutomu Tamura
Foundation for Promotion of
Japanese Aerospace Technology
1-16-6 Izumi-Chuo, Izumi-ku, Sendai,
Miyagi 981-3133, Japan
tamura.tsutomu@jaxa.jp

Mamoru Oike
Ishinomaki Senshu University
1 Shinmito, Minamisakai, Ishinomaki,
Miyagi 986-8580, Japan
oike@isenshu-u.ac.jp

ABSTRACT

Temperature depression in a cavitating orifice flow was experimentally investigated with liquid nitrogen in order to clarify the influence of turbulent flow around a bubble on thermodynamic effects on cavitation. The temperature began to decrease at the outlet of the orifice when the cavitation number decreased below 0.84. Moreover, the temperature depression became larger as the cavitation number became smaller. In addition, the temperature depression also became greater as the flow velocity became lower when the cavitation numbers were equal. Based on theoretical considerations and experimental results, the difference of temperature depression can be considered to be caused by the enhancement of thermal transport around bubbles due to the turbulent flow. In addition, if thermal transport is enhanced as mentioned above, the temperature in the area where the cavitation collapses can become higher than that upstream of the orifice due to the temporary breakdown of the heat balance between the inception and collapse of cavity bubbles.

INTRODUCTION

Temperature depression around bubbles is an indicator of the thermodynamic effects on cavitation. When cavity bubbles occur and grow the temperature around the bubbles decreases due to the latent heat of evaporation. Consequently, the saturated vapor pressure around the bubbles decreases and the growth of the bubbles should be delayed.

Therefore, the thermodynamic effects improve the performance of a rocket turbopump inducer and suppress cavitation instabilities such as cavitation surge and rotating cavitation [1] because the thermodynamic effects strongly act in cryogenic fluids. Furthermore, if the thermodynamic effects properly affect cavitation in cryogenic inducers, the performance of the inducers can be further improved. However, a more appropriate model of the thermodynamic effects should be constructed to improve the design approach of inducers because the conventional models are limited in its estimation of the degree of the thermodynamic effects.

Equation (1) denotes a simple heat balance around a cavity bubble:

$$\alpha\rho_{\mathrm{V}}L=(1-\alpha)\rho_{\mathrm{L}}C_{p,\mathrm{L}}\Delta T. \quad (1)$$

Then, the following *B*-factor (dimensionless temperature depression) was introduced from Eq. (1) by Stepanoff [2]:

$$B=\frac{\alpha}{1-\alpha}=\frac{\Delta T}{T^{*}},\quad T^{*}=\frac{\rho_{\mathrm{V}}L}{\rho_{\mathrm{L}}C_{p,\mathrm{L}}}. \quad (2)$$

Equations (1) and (2) assume that evaporative latent heat required for the inception of a cavity bubble is obtained from the whole liquid around the bubble. However, the latent heat is generally obtained from the liquid near the bubble. Moreover, the thermal transport around bubbles should be strongly affected by the turbulent property. Therefore, constructing an advanced model for the thermodynamic effects on cavitation requires the elucidation on the turbulent property around cavity bubbles.

Hord et al. [3-6] conducted experiments on several cryogenic cavitating flows (i.e. hydrofoil, venturi, ogive,) with liquid hydrogen and liquid nitrogen. They compared the mean cavity length and the temperature distribution in the cavity by visualization tests. Billet et al. [7] proposed an empirical formula for the estimation of the *B*-factor by using the experimental results by Hord. Franc et al. [8] conducted experiments on an inducer with the R-114 refrigerant and estimated the *B*-factor based on the difference of cavitation number between water and R-114. Yoshida et al. [9] also estimated the *B*-factor of an inducer based on the difference of cavitation number between water and liquid nitrogen. Moreover, Brennen [10] proposed a Σ-parameter based on thermal conduction around a single bubble, Kato [11] proposed an α-parameter and Watanabe et al. [12] proposed a Σ^*-parameter in consideration of thermal conduction near a sheet cavity. However, the relation between the thermodynamic effects and the turbulent property around bubbles has not yet been clarified.

Therefore, experiments on a cryogenic cavitating flow occurring at the outlet of a circular plate orifice were conducted with liquid nitrogen in order to clarify the influence of the turbulent property around cavity bubbles on the thermodynamic effects on cavitation. In the present study, the correlation between the heat transfer coefficient and the turbulent intensity in the cavitating flow was investigated experimentally and numerically.

EXPERIMENTAL FACILITY

Experiments were conducted in the Cryogenic Cavitation Tunnel [13] at the JAXA Kakuda Space Center. Figure 1 shows a schematic diagram and Fig. 2 shows a view of this tunnel in an experiment. The working fluid is liquid nitrogen, which flows from the run tank to the catch tank through the test section. The cavitation number in the test section is controlled by pressure in the run tank and opening of the flow control valve downstream of the test section. Volumetric flow rate is measured by a turbine flowmeter upstream of the test section.

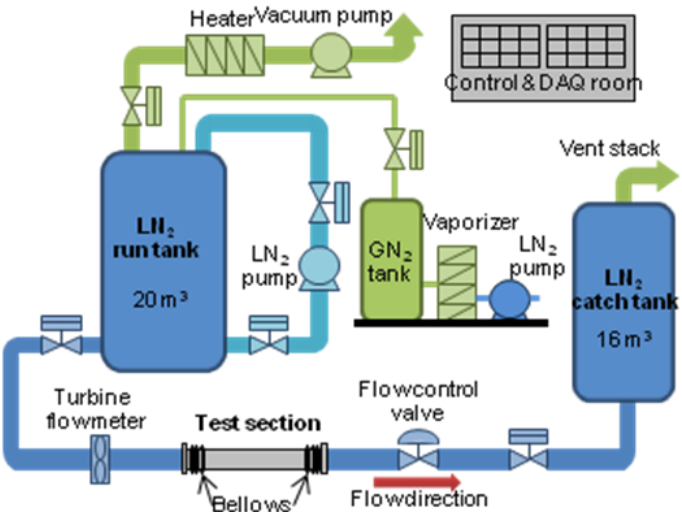

Fig. 1 Schematic diagram of cryogenic cavitation tunnel.

Fig. 2 View of cryogenic cavitation tunnel.

Figure 3 shows a schematic diagram of the test section, which has a circular orifice plate. The inner diameter of the test section is 83.1 mm and the hole diameter of the orifice is 35.0 mm. There are a measurement point upstream of the orifice (location ①) and more four measurement points downstream of the orifice (location ②-⑤). The distances of the latter measurement points from the orifice are x/D = 2.11, 3.54, 4.97, and 7.83, respectively. Each measurement point has a pressure sensor and a thermocouple. In addition, the temperature probe shown in Fig. 4 was installed at the inlet and the outlet of the orifice (location ① and ②) in order to accurately measure the temperature depression in cavitating flow. This temperature probe has a DT-670-SD silicon diode sensor glued on the tip of the stainless tube, and the sensor was set at the center of the mainstream. The sensor is manufactured by Lakeshore Cryotronics Inc. and is 3.2 mm in length, 1.9 mm in width and 1.1 mm in height, and has a temperature accuracy of ± 22 mK at 77 K.

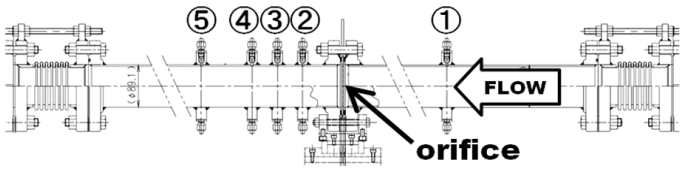

Fig. 3 Schematic diagram of test section and measurement points (locations ①-⑤).

Fig. 4 Temperature probe with DT-670-SD silicon diode sensor.

Experiments were conducted with the flow control valve being opened step by step at a constant pressure in the run tank. The pressure in the run tank was set at 0.5 MPa in test 1 and at 0.9 MPa in test 2, and the inlet temperature of the orifice was 79 K in both tests. Pressure, temperature and volumetric flow rate were stored to a digital data recorder at 50 Hz.

EXPERIMENTAL RESULTS

Figure 5 shows evolutions of the cavitation number, σ, and the temperature depression, ΔT_D (= T_{D1} - T_{D2}), measured with the temperature probe in test 1.

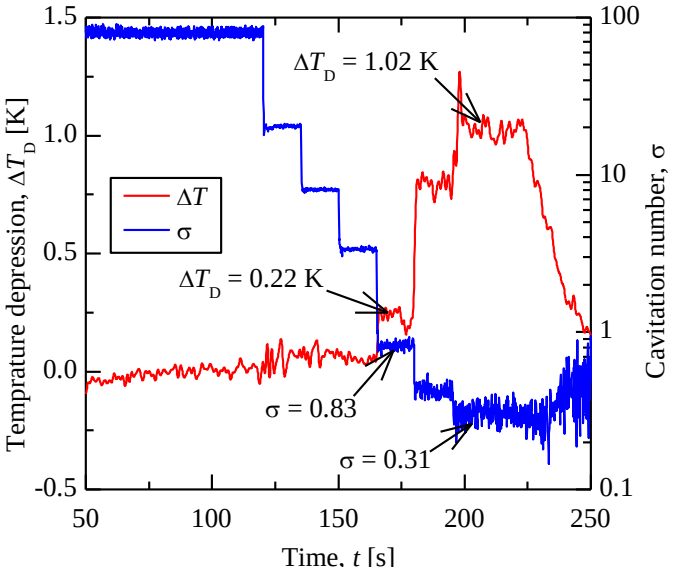

Fig. 5 Evolutions of cavitation number and temperature depression at the outlet of orifice (test 1: P_{RUN} = 0.5 MPa, T_{D1} = 79 K).

The horizontal axis denotes the time, t, the vertical axis on the left denotes the temperature depression, ΔT_D, and the vertical axis on the right denotes the cavitation number, σ, calculated by the following equation.

$$\sigma = \frac{2\{p_2 - p_{SV}(T_{D1})\}}{\rho_L U_{TH}^2} \quad (3)$$

The temperature depression began to increase when the cavitation number was 0.83 and it became larger as the cavitation number became smaller. The maximum temperature depression was about 1.02 K when the cavitation number was at the minimum (σ = 0.31).

The evolutions of the cavitation number and the temperature depression in test 2 were quite similar to those in test 1. However, the maximum temperature depression in test 2 was about 0.90 K, which was smaller than that in test 1 even if the minimum cavitation number was almost equal (σ ≈ 0.3).

Figure 6 shows the comparison of the B-factor with increase of the flow velocity, U_{TH}, at the orifice throat in two tests.

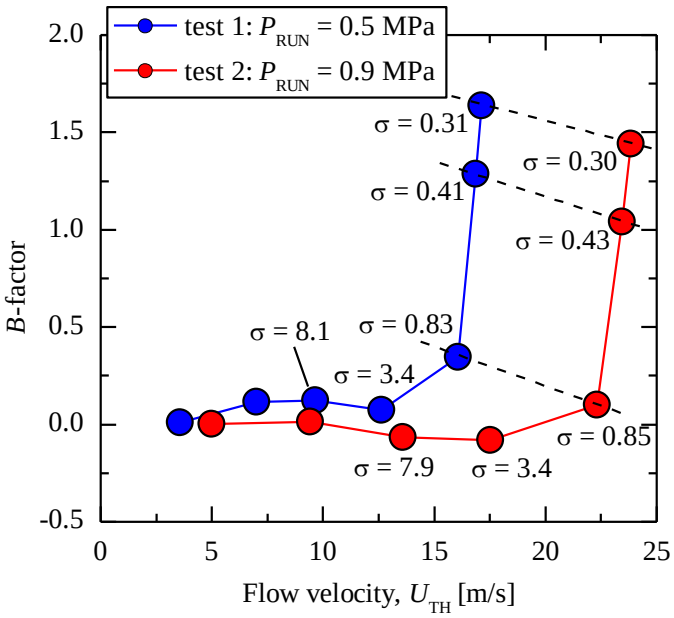

Fig. 6 B-factor corresponding to flow velocity.

The B-factor was calculated by Eq. (2). In both tests, the B-factor increased as the cavitation number decreased, which is considered to be caused by an increase in the void fraction of cavity bubbles. Furthermore, the B-factor became smaller as the flow velocity, U_{TH}, became higher in the comparison of two cases that the cavitation number was almost equal below 0.83, as described by broken lines in Fig. 6. The aspect of a cavitating flow with the same cavitation number is expected to be similar to each other even if the flow velocity differs. Therefore, the B-factor was considered to be varied not only by the void fraction but also by the flow velocity.

DISCUSSION

INFLUENCE OF TURBULENT FLOW ON TEMPERATURE DEPRESSION

From a simple consideration based on bubble dynamics, the influence of the turbulent intensity around a bubble on the temperature depression in a cavitating flow is considered.

The heat balance around a bubble can be described as follows.

$$\rho_V L \frac{d}{dt}\left(\frac{4}{3}\pi R^3\right) = 4\pi R^2 \dot{q} \quad (4)$$

The heat flux, $\dot{q}$, shown in Eq. (4) is described by Eq. (5) with the turbulent heat transfer coefficient, h_T, from the bubble surface to the surrounding flow:

$$\dot{q} = h_T \Delta T \,. \quad (5)$$

Combining Eq. (5) with Eq. (4), temperature depression, ΔT, around a bubble is described by Eq. (6):

$$\Delta T = \frac{\rho_V L}{h_T}\dot{R}. \quad (6)$$

Here, the speed of bubble's growth, $\dot{R}$, is described by Eq. (7) from the simplified Rayleigh-Plesset equation [14]:

$$\dot{R} = U_{TH}\sqrt{-\frac{1}{3}\left(\sigma + C_f\right)}. \quad (7)$$

Then, Eq. (8) is introduced by combining Eqs. (2), (6), and (7).

$$B = \frac{\rho_L C_{p,L} U_{TH}}{h_T}\sqrt{-\frac{1}{3}\left(\sigma + C_f\right)} \quad (8)$$

Equation (8) shows that the *B*-factor is expected to increase with an increase in flow velocity, U_{TH}, a decrease in cavitation number, σ, or a decrease in turbulent heat transfer coefficient, h_T. This seems to conflict with the experimental result shown in Fig. 6. However, the turbulent heat transfer coefficient around a bubble is strongly affected by the turbulent intensity in the flow, and then it can be considered as a function of Reynolds number. Therefore, the *B*-factor was considered to be depressed by the increase in the turbulent heat transfer coefficient due to an increase in the Reynolds number.

Figure 7 shows the turbulent heat transfer coefficient, h_T, based on Eq. (8) and experimental results.

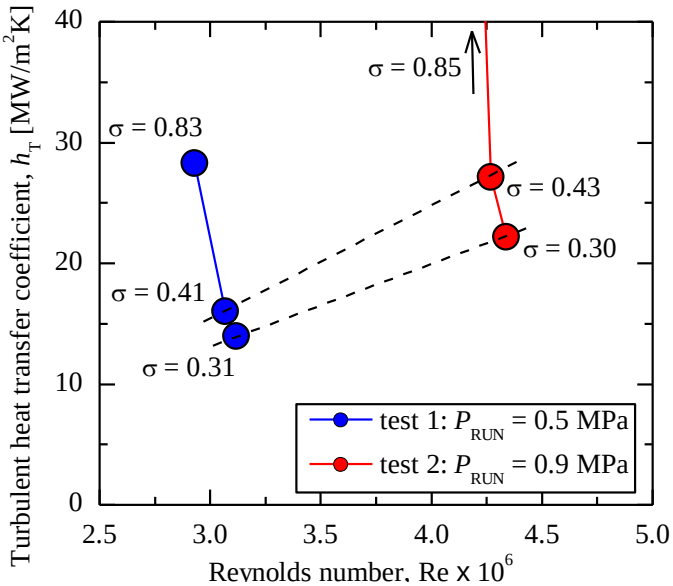

Fig. 7 Turbulent heat transfer coefficient corresponding to Reynolds number.

Here, the cavitation number, σ, calculated by Eq. (3) and the pressure coefficient, C_f, calculated by the Bernoulli equation between the upstream and the throat of the orifice (C_f = -0.968) were used for the estimation of the turbulent heat transfer coefficient, h_T.

From Fig. 7, it can be seen that the turbulent heat transfer coefficient, h_T, decreases as the cavitation number, σ, decreases in both cases and increases as the Reynolds number, Re, increases, even if the cavitation numbers, σ, were almost equal, as described by broken lines.

When the cavitation numbers are equal, the void fraction is expected to hardly vary. However, because the turbulent intensity increases due to an increase of the Reynolds number, the thermal transport should be enhanced and the heat transfer coefficient results in increasing.

On the other hand, when the cavitation number decreases, the void fraction also increases. Then, by analogy with a bubbling flow [15], the turbulent intensity can be considered to decrease in the cavitating flow. Consequently, the turbulent heat transfer coefficient should be depressed with decrease in the cavitation number, as shown in Fig. 7.

In order to clarify the correlation among void fraction, turbulent intensity and turbulent heat transfer coefficient, a numerical analysis was conducted. Figure 8 shows a typical aspect of the cavitating orifice flow under the same condition as that in test 1 by Front Flow/Blue [16].

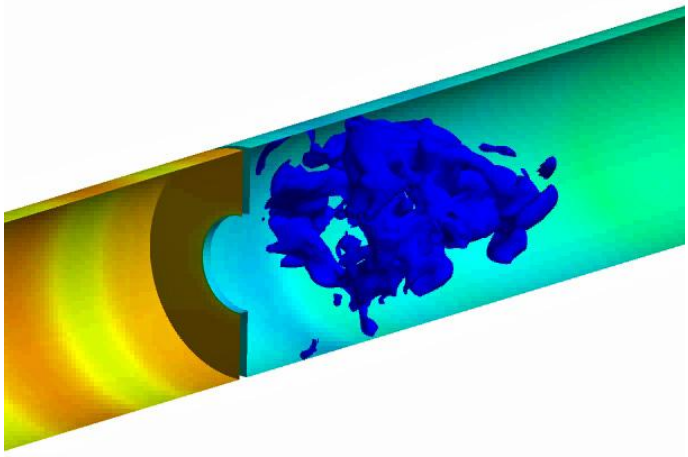

Fig. 8 Aspect of cavitating flow by numerical analysis (test1: σ = 0.3).

Thermodynamic effects on cavitation were neglected in the cavitation model of this calculation. Cavity bubbles are described as blue contour surfaces where the void fraction is 30 % and it occurs in the vortex ring at the outlet of the orifice and gradually collapsed downstream.

Table 1 shows the turbulent intensity and the mean void fraction by the numerical analysis and the heat transfer coefficient and the *B*-factor by the experimental analysis.

Table 1 Results of experimental and numerical analysis.

	case 1 (test 1)	case 2 (test 2)	case 3 (non-cavitation)
σ	0.3	0.3	-
Re	3.1×10^6	4.3×10^6	3.1×10^6
<u'> (CFD)	0.45	0.77	0.62
<α> (CFD)	1.4 %	3.9 %	0.0
h_T (EXP)	14×10^6	20×10^6	-
B (EXP)	1.7	1.45	-

CFD: Numerical results with Front Flow/Blue
EXP: Experimental results

Case 1 was conducted under the condition of test 1 (σ = 0.3,) case 2 was conducted under that of test 2 (σ = 0.3,) and case 3 was conducted under the condition without cavitation. The turbulent intensity and the mean void fraction were calculated at the same point measured in the experiment. Here, although the void fraction in case 2 is slightly larger than that in case 1, the difference in the void fraction in both cases should be neglected because the accuracy in averaging the void fraction strongly depends on its location.

The influence of the turbulent flow on the *B*-factor can be considered as follows:

1) Comparison of case 1 and 2 shows that the turbulent intensity in a cavitating flow increased as the Reynolds number increased with constant cavitation number. The heat transfer coefficient then increased and the *B*-factor decreased. Therefore, it can be considered that the *B*-factor in a cavitating flow is depressed due to an increase in the turbulent intensity as the Reynolds number increases.
2) Comparison of case 1 and 3 shows that the turbulent intensity decreased with an increase in the void fraction. The difference in these cases is only the presence of cavitation. Therefore, it can be considered that the turbulent intensity in a cavitating flow is depressed due to the presence of cavity bubbles and then the turbulent heat transfer coefficient is also depressed.

Finally, it can be concluded that the *B*-factor increase not only by a decrease in the cavitation number but also by a decrease in the turbulent intensity of the mainstream.

INFLUENCE OF TURBULENT FLOW ON CAVITY GROWTH

Figure 9 shows a distribution of the *B*-factor measured by thermocouples at the locations ②-⑤. The location numbers shown in Fig. 9 correspond to those shown in Fig. 3, respectively.

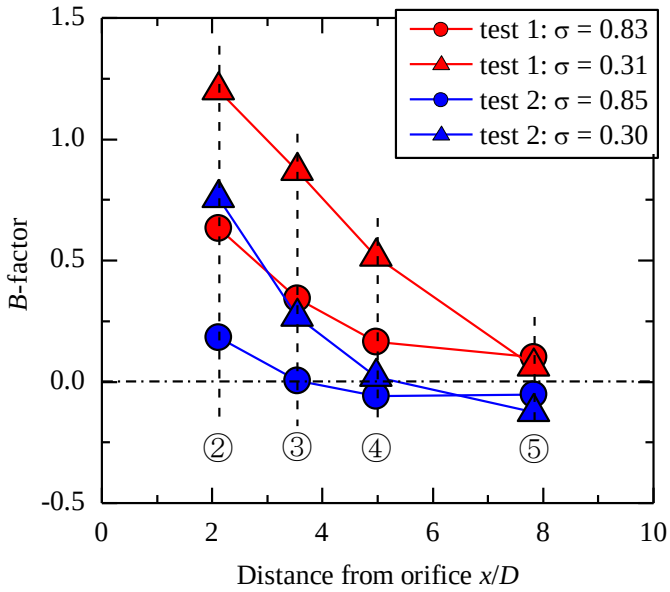

Fig. 9 Distributions of *B*-factor downstream of orifice.

In any case, the *B*-factor decreases as the distance from the orifice increases, which is considered to be caused by the latent heat of condensation due to the collapse of the cavity bubbles.

Comparison of results with the different cavitation numbers in the same test shows that the *B*-factor increased overall due to the increase in the void fraction of cavity bubbles as the cavitation number decreased.

Furthermore, comparison of results with the same cavitation number in the different tests shows that the *B*-factor in test 1 was larger than that in test 2. This was considered to be caused by an increase in the turbulent intensity as mentioned above.

Meanwhile, the *B*-factor at the location ⑤ in test 2 (σ = 0.30) was slightly below zero. This means that the temperature measured at the location ⑤ was higher than that measured at the location ①. This can be considered as follows.

When cavitation occurs, the temperature should be decreased by the latent heat of evaporation, Q_E. In contrast, when cavitation collapses, the temperature should be increased by the latent heat of condensation, Q_C. Because the heat quantities of evaporation and condensation should balance, the temperature after collapse is expected to be equal to that before inception if the thermal diffusivity in the cavitating flow is adequately small. This heat balance can be described as follows with an assumption that thermal transport is stationary.

$$-Q_E + Q_C = 0 \quad \Rightarrow \quad T_{before} \approx T_{after} \qquad (9)$$

However, if the turbulent intensity around cavity bubbles is quite large, the heat balance can be considered to be temporarily broken. The temperature depression is decreased in cavitating flow where the turbulent intensity is large, as mentioned above. Then, the additional heat, Q_T, can be considered to be supplied to near the bubbles surface by the turbulent flow. After that, cavity bubbles begin to collapse, and

the temperature gradually increases due to the latent heat of condensation. When all cavity bubbles collapse, the temperature might temporarily exceed that before inception due to the additional heat. This can be also described as follows.

$$-Q_{\mathrm{E}} + Q_{\mathrm{T}} + Q_{\mathrm{C}} > 0 \quad \Rightarrow \quad T_{\mathrm{before}} < T_{\mathrm{after}} \qquad (10)$$

In test2, the large amount of additional heat was expected to be supplied from the mainstream to the bubbles surface because the turbulent heat transfer coefficient in test 2 is larger than that in test 1. Then, the temperature at the location ⑤ was considered to exceed that at the location ①. This temperature "rise" is expected to delay the "shrink" of cavity bubbles, which can be considered to be a harmful aspect of the thermodynamic effects on cavitation.

In addition, because the turbulent thermal transport is not stationary, more adequate comprehensions of cavitating turbulent flow and its thermal transport mechanism have to be required. Now, authors are preparing for a visualization of cryogenic cavitating flow in order to compare the temperature depression with the aspect of cavitating turbulent flows.

CONCLUSION

Experimental and numerical investigations on temperature depression in a cavitating orifice flow were conducted with liquid nitrogen in order to clarify the influence of the turbulent flow on the thermodynamic effects on cavitation. The results can be summarized as follows:

(1) The temperature depression in the cavitating flow increased with the decrease in the cavitation number or the flow velocity.
(2) From a theoretical consideration, *B*-factor is considered to increase with a decrease in cavitation number, a decrease in turbulent heat transfer coefficient, or an increase in flow velocity.
(3) From the experimental and numerical analyses, it was considered that the turbulent heat transfer coefficient in the cavitating flow was reduced by the increase in the void fraction but increased by the enlargement of the turbulent intensity.
(4) Although the thermodynamic effects generally reduce the temperature in the area where cavity bubbles occur, the present results showed that the thermodynamic effects could increase the temperature in the area where the bubbles collapsed when the turbulent intensity was large.

Then, it can be concluded that the thermodynamic effects affect on cavitation either favorably or unfavorably. They can usually suppress and delay the development of cavity bubbles. However, if the cavitating flow has the large turbulent intensity, the shrink of cavity bubbles may be delayed by the thermodynamic effects.

NOMENCLATURE

B Stepanoff's *B*-factor
C_f pressure coefficient
C_p specific heat capacity [J/kg·K]
D hole diameter of orifice [m] = 0.035 mm
L latent heat [J/kg]
Q volumetric flow rate [m^3/s], heat quantity [J]
R bubble radius [m]
$\dot{R}$ speed of bubble's growth [m/s]
Re Reynolds number = $\rho_V D U_{TH}/\mu_L$
T temperature [K]
T^* characteristic temperature [K] = $\rho_V L/\rho_L C_{p,L}$
U flow velocity [m/s]
h heat transfer coefficient [W/m^2·K]
p pressure [Pa]
$\dot{q}$ heat flux [W/m^2]
u' turbulent intensity [m/s]
x distance from the orifice [m]
ΔT temperature depression [K]
α void fraction
μ viscosity [m^2/s]
ρ density [kg/m^3]
σ cavitation number

Subscripts:

C by condensation
D measured by diode temperature probe
E by evaporation
L liquid state
SV saturated state
T by turbulence
TH at the orifice throat
V vapor state
number indicator of measurement locations

REFERENCES

[1] Kikuta, K., Yoshida, Y., Watanabe, M., Hashimoto, T., Nagaura, K. and Ohira, K., 2008, "Thermodynamic Effect on Cavitation Performance and Cavitation Instabilities in an Inducer," J. Fluids Eng., **130**, 111302.
[2] Stepanoff, A. J., 1964, "Cavitation Properties of Liquids," J. Eng. Power, **80**, pp.195-200.
[3] Hord, J., Anderson, L. M. and Hall, W. J., 1972, "Cavitation in Liquid Cryogens: I-Venturi," NASA CR-2054.
[4] Hord, J., 1973, "Cavitation in Liquid Cryogens: II-Hydrofoil," NASA CR-2156.
[5] Hord, J., 1973, "Cavitation in Liquid Cryogens: III-Ogives," NASA CR-2242.
[6] Hord, J., 1974, "Cavitation in Liquid Cryogens: IV-Combined Correlations for Venturi, Hydrofoil, Ogives, and Pumps," NASA CR-2448.
[7] Billet, M. L., Holl, J. W., Weir, D. S., 1981, "Correlations of Thermodynamic Effects for Developed Cavitation," J. Fluids Eng., **103**, pp.534-542.
[8] Franc, J. P., Rebattet, C. and Coulon A., 2004, "An Experimental Investigation of Thermal Effects in a Cavitating Inducer," J. Fluids Eng., **126**, pp.716-723.
[9] Yoshida, Y., Kikuta, K., Hasegawa, S., Shimagaki, M., and Tokumasu, T., 2007, "Thermodynamic Effects on a Cavitating Inducer in Liquid Nitrogen," J. Fluids Eng., **129**, pp.273-278.

[10] Brennen, C. E., 1973, “The Dynamic Behavior and Compliance of a Stream of Cavitating Bubbles,” J. Fluids Eng., **95**(4), pp.533-541.
[11] Kato, H., 1984, “Thermodynamic Effect on Incipient and Development of Sheet Cavitation,” *Proceedings of International Symposium on Cavitation Inception*, New Orleans, LA, Dec. 9-14, ASME FED., 16, pp.127-136.
[12] Watanabe, S., Hidaka, T., Horiguchi, H., Furukawa, A. and Tsujimoto, Y., 2007, “Steady Analysis of the Thermodynamic Effect of Partial Cavitation Using the Singularity Method,” J. Fluids Eng., **129**(2), pp.121-127.
[13] Niiyama, K., Yoshida, Y., Hasegawa, S., Watanabe, M., Hashimoto, T., Shimagaki, M., Kikuta, K., Nagaura, K., and Tamura, T., 2008, “Verification Test Results for the Cryogenic Cavitation Tunnel in JAXA,” JAXA RM-08-008 (in Japanese).
[14] Brennen, C.E., 1995, *Cavitation and Bubble Dynamics*, Oxford University Press, New York, U.S., Chap. 2.
[15] Sato, Y., Sadatomi, M., and Sekoguchi, K., 1981, “Momentum and Heat Transfer in Two-phase Bubble Flow I-Theory,” Int. J. Multiphase Flow, **7**, pp.167-177.
[16] Guo, Y., Kato, C., and Yamade, Y., 2006, “Basic Features of the Fluid Dynamics Simulation Software “Front Flow/Blue”,” Seisan-kenkyu, 58, pp.11-15.